The Knee 26 (2019) 302–309

Contents lists available at ScienceDirect

The Knee

Morphology of the patellar tendon and its insertion sites using three-dimensional computed tomography: A cadaveric study

Ryunosuke Oikawa [a], Goro Tajima [a,*], Jun Yan [b], Moritaka Maruyama [a], Atsushi Sugawara [a], Shinya Oikawa [a], Takaaki Saigo [a], Hirotaka Takahashi [a], Minoru Doita [a]

[a] Department of Orthopaedic Surgery, Iwate Medical University, Iwate, Japan
[b] Department of Anatomy, Iwate Medical University, Iwate, Japan

ARTICLE INFO

Article history:
Received 10 May 2018
Received in revised form 30 September 2018
Accepted 5 December 2018

Keywords:
Anterior cruciate ligament reconstruction
Bone–patellar tendon–bone graft
Insertion
Morphology
Patellar tendon

ABSTRACT

Background: To clarify, with three-dimensional (3D) images, the morphological properties of the patellar tendon and both of its insertion sites.
Methods: Thirty-two human cadaveric left knees were evaluated, and 3D computed tomography images were created. These images were used to analyse the morphology of both insertion sites of the patellar tendon, and the width, length and thickness of each region of the patellar tendon.
Results: The insertion sites of the patellar tendon on the patellar and tibial sides were V-shaped and crescent-shaped, respectively, with the respective bony apexes located at 44.5 ± 2.2% (standard deviation) and 35.5 ± 2.8% of the tendon width from its medial edge. The proximal, central and distal widths of the patellar tendon were 29.9 ± 2.7 mm, 27.3 ± 2.5 mm and 25.0 ± 2.4 mm, respectively. The length of the patellar tendon was shortest at 40.6% ± 6.7% of the central width and gradually became longer toward both edges. The patellar tendon was thickest in the central portion of 40–75% and gradually became thinner toward both edges.
Conclusions: The morphological properties of the patellar tendon and its insertion sites on both the patellar and tibial sides were consistent. These findings indicate that the characteristics of the bone–patellar tendon–bone graft markedly depend on the location from which it is harvested, and that these characteristics contribute to predicting the length, width and shapes of the bone plugs of the graft when performing bone–patellar tendon–bone surgery.

1. Introduction

Using a bone–patellar tendon–bone (BTB) graft to reconstruct a torn anterior cruciate ligament (ACL) has been recognised as a successful procedure that produces good clinical results [1–3]. The advantages of the BTB graft include a high degree of initial tensile strength and stiffness [4,5], rigid fixation using the interference screw technique [6], and direct bone-to-bone healing [7]. However, graft–tibial tunnel length mismatch is a well-known intraoperative complication in BTB ACL reconstruction [8–11]. This mismatch occurs when the relative length of the BTB graft construct exceeds the combined length of the femoral tunnel, intra-articular ACL distance, and tibial tunnel length. The tibial bone plug is consequently located outside the tibial tunnel. If an inadequate amount of the tibial bone plug lies within the tibial tunnel, graft fixation may be compromised [12].

Various intraoperative techniques, including graft rotation and the bone block technique, have been proposed to manage graft–tunnel mismatch in BTB ACL reconstruction. However, each technique comes with potential disadvantages such as compro-

* Corresponding author at: Department of Orthopaedic Surgery, Iwate Medical University, 19-1 Uchimaru, Morioka, Iwate 020-8505, Japan.
E-mail address: goro.t@triton.ocn.ne.jp. (G. Tajima).

https://doi.org/10.1016/j.knee.2018.12.002
0968-0160/

mised fixation, graft strain, and low technical feasibility [9–11,13–17]. Therefore, it is preferable to avoid mismatch in the first place [18]. Several studies have investigated the relationship between the length of the tibial tunnel and angle of the tibial guide [11,16,19]. Additionally, pre-operative assessment using magnetic resonance imaging (MRI) has been recognised as a valuable tool to estimate the tendon length of the BTB graft [12,20].

The central third of the patellar tendon is the portion normally used for ACL reconstruction, regardless of whether it is an autograft or allograft. However, because the inferior patella is V-shaped there is marked variability in predicting the length of the BTB graft based on the location from which it is harvested. Basso et al. reported that the patellar inferior apex was not located at the midpoint of the width of the patellar tendon, but tended to lie medial to the midpoint; however, details of the tibial insertion site remain unclear [21]. To avoid graft tunnel mismatch, it is necessary to define the characteristics of the insertion sites of the patellar tendon on both the patellar and tibial sides; this information could then be used to predetermine the length of the BTB graft. Furthermore, a detailed understanding of the patellar tendon may help to characterise the regional morphological properties of the BTB graft.

Excellent biomechanical and clinical results have recently been reported using an anatomic rectangular ACL reconstruction method that uses a BTB graft with parallelepiped bone plugs that mimic the orientation of the native ACL fibres and their junctions [22–26]. To perform anatomical ACL reconstruction using the BTB graft with these new techniques, it is necessary to define the morphology of the patellar tendon and both bone–tendon junctions.

The purpose of the present study was to clarify the characteristics of the patellar tendon and its insertion sites using three-dimensional (3D) images. It was hypothesised that the characteristic features of both the tendon and its insertion sites can be identified and that they are consistent.

2. Materials and methods

2.1. Specimen preparation

Thirty-two unpaired human cadaveric knees (19 male and 13 female specimens; age range, 62–87 years; mean age, 76.8 ± 7.4 years) with no severe macroscopic degenerative or traumatic changes were used in the present study. All cadavers were fixed in 10% formalin and preserved in 50% alcohol for six months. The present cadaveric study was approved by the institutional review board (IRB: H27-99). Preparation began with removal of the skin and soft subcutaneous tissue on the anterior side of the knee. The medial and lateral retinaculae and the paratenon overlying the anterior side of the patellar tendon were removed, allowing easier identification of the lateral and medial edges of the patellar tendon and better definition of the patellar tendon. After the patellar tendon was identified, the anterior side of the tendon was grossly observed and the distal peripheral line of the tibial insertion site was identified.

The quadriceps tendon was transected at the junction with the proximal edge of the patella. The fat pad and synovium were removed from the posterior aspect of the tendon, and then the posterior patellar insertion site of the patellar tendon and the proximal peripheral line of the tibial insertion site of the patellar tendon were observed and defined. The tibia was transected at the middle portion of the bone shaft. Hence, the dissection produced a patella–patellar tendon–tibia complex that was isolated from the specimen.

2.2. Three-dimensional visualisation and measurements

The specimen was placed in a custom-made traction device (Figure 1), and the tibial bone was fixed to the base of the device. In each knee, the patellar bone was proximally grasped with tenaculum forceps, and an approximately 10-N load was then gently applied through a string structure with a tension gauge to the patellar bone to keep its tendon taut and aligned with the shaft of the tibia.

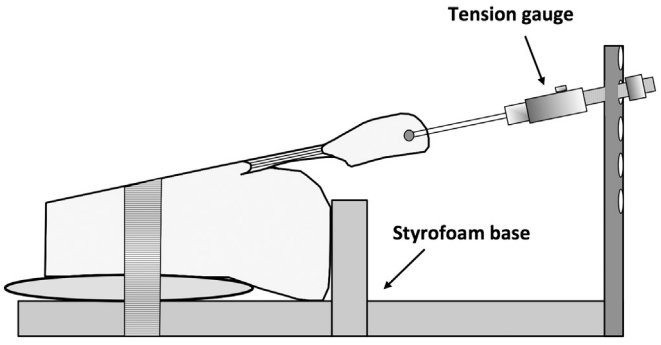

Figure 1. Schematic of a custom-made traction device. The tibia was fixed to the base of the device. The patellar tendon was towed with a constant 10-N load through a string structure with a tension gauge and aligned with the shaft of the tibia.

This complex was scanned using a 16-row multislice computed tomography (CT) scanner (ECLOS; Hitachi Medical Corporation, Tokyo, Japan). Axial-plane images with 0.5-mm slices were obtained and saved as Digital Imaging and Communications in Medicine data. All digital imaging data were uploaded to dedicated software (Mimics version 19.0; Materialise N.V., Leuven, Belgium), and accurate 3D models of the specimens, including each segment of the bone and tendon, were created. A segmentation technique was then applied to each CT mask to identify and separate the patellar tendon from the bones and surrounding residual soft tissue [27,28]. The data from the 3D model were uploaded to advanced analysis software (3-matic version 15.0; Materialise N.V.).

The characteristics of the insertion sites of the patellar tendon were analysed using the 3D model, which consisted of bone and a translucent patellar tendon. The areas of the insertion sites of the patellar tendon, and the width, length and thickness of the patellar tendon were also calculated. The width of the patellar tendon was measured directly from the medial to lateral borders. The proximal, distal, and central widths were measured at the apex of the inferior patellar pole, at the vertex of the proximal boundary of the insertion site on the tibial side, and at their respective midpoints (Figure 2a). The length of the patellar tendon between the inferior patellar edge and the superior edge of the tibial insertion site of the patellar tendon was measured at every 10% interval of the central width of the patellar tendon from its medial edge, and the shortest position was detected and measured (Figure 2a). The thickness of the patellar tendon was also measured at every five percent interval of the central width of the patellar tendon from its medial edge (Figure 3a). These measurements were performed using specific software (3-matic version 15.0; Materialise N.V.) [29]. The accuracies of the length and area measurements were <0.1 mm and 0.1 mm^2, respectively. When comparing the accuracy of the 3D models generated from CT data with the optical scan, the average error was 0.65 ± 0.31 mm or around one third of the pixel size [30].

2.3. Statistical analysis

Analyses were performed using SPSS software (version 22.0; IBM, Armonk, NY, USA) with significance for all analyses set at $P < 0.05$. The distribution of each variable was checked for normality using the Kolmogorov–Smirnov test. Statistical analysis included repeated measures analysis of variance with Tukey's post hoc test for continuous data of tendon regions.

3. Results

3.1. Macroscopic findings and three-dimensional analysis of the characteristics of the insertion sites of the patellar tendon

3.1.1. Patellar tendon insertion site on the patellar side

Macroscopic examination showed that the anterior superficial fibres of the patellar tendon were continuous over the patella with the tendon of the quadriceps femoris (Figure 4a). The posterior superficial fibres of the patellar tendon were clearly attached to the inferior patella (Figure 4b). It was difficult to define the surface area of the insertion site of the patellar tendon on the

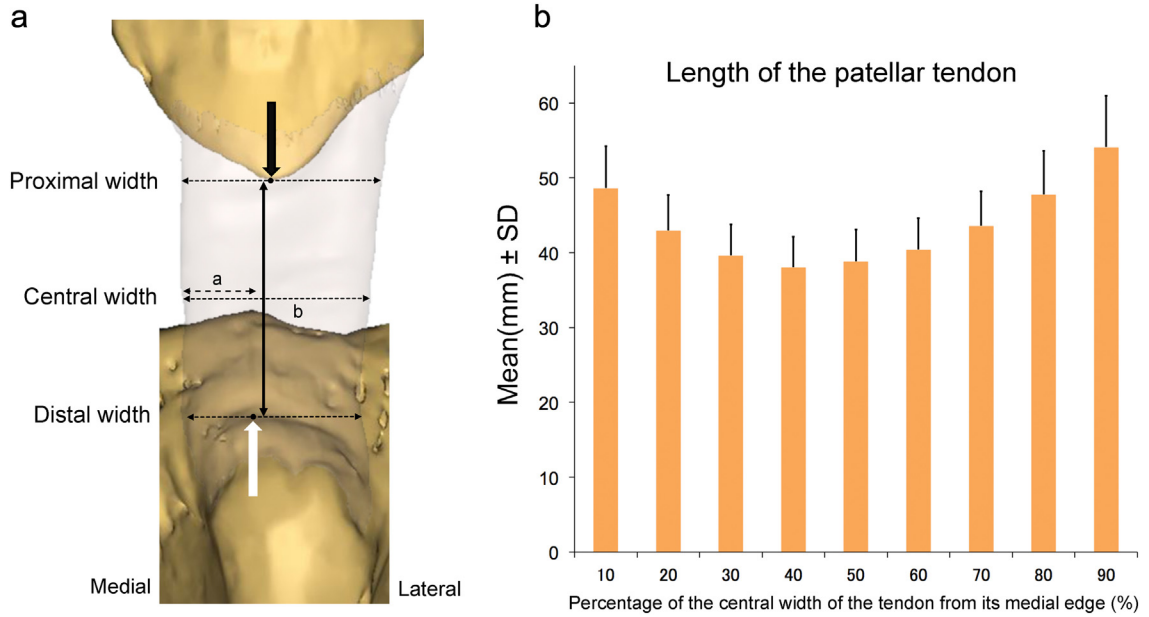

Figure 2. Three-dimensional image of the knee and column graph showing the length of the patellar tendon. a. Anterior view. This view was used for each measurement in the current study. The black arrow indicates the apex of the inferior pole of the patella. The white arrow indicates the vertex of the arcuate groove of the tibia. The position of the shortest length of the tendon is represented as *a*/*b*. b. The length of the patellar tendon was shortest at a location 40% medial of the central width; the lateral side was longer than the medial side, which gradually became longer toward both edges.

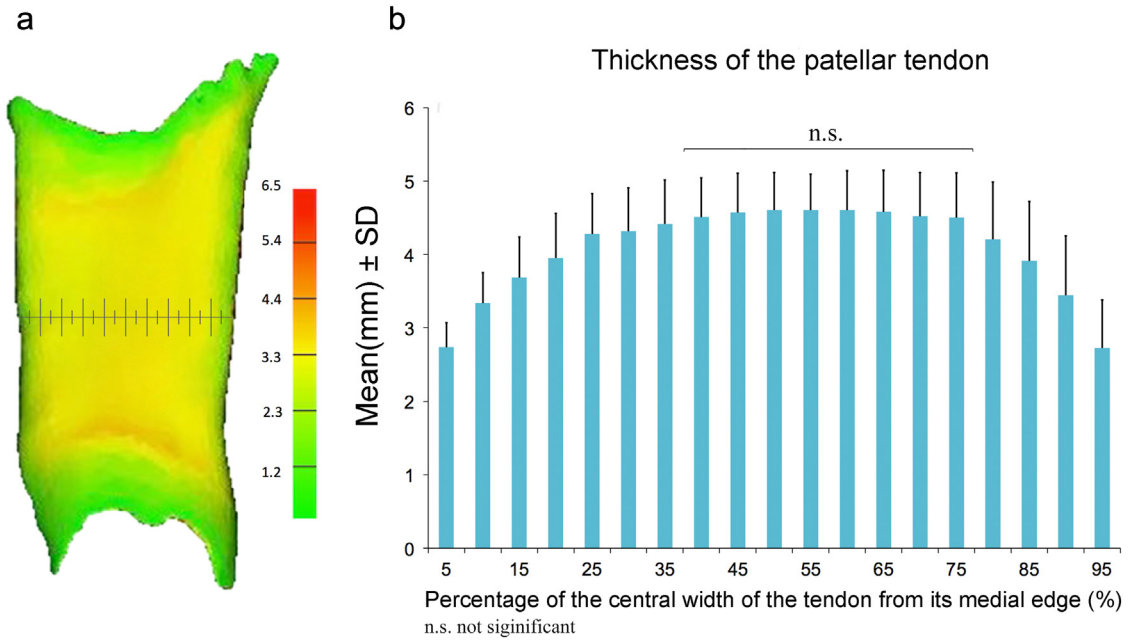

Figure 3. Colour representation and column graph indicating the patellar tendon thickness. a. The thickness of the patellar tendon was analysed using specific software (3-matic version 15.0; Materialise N.V., Leuven, Belgium). The colour represents the thickness of the tendon, with red indicating thick regions and green indicating thin regions. b. The thickness of the patellar tendon did not significantly differ in the range of 40–75% from the medial edge ($P = 0.051$). (For interpretation of the references to colour in this figure legend, the reader is referred to the web version of this article.)

patellar side because the anterior superficial fibres were widely spread and continuous with the superficial fibres of the quadriceps tendon. In the 3D analysis, the patellar tendon surrounded the inferior edge of the patella (Figure 4c and d), and the apex of the inferior pole of the patella was 44.5 ± 2.2% of the proximal width of the patellar tendon from its medial edge (Figure 2a). Quantitative data are summarised in Table 1.

3.1.2. Patellar tendon insertion site on the tibial side

Macroscopic examination showed that the proximal boundary of the insertion site of the patellar tendon corresponded with the arcuate groove, which began at the upper medial corner of the tibial tuberosity, extended to, and turned distally along the lateral side of the tibial tuberosity (Figure 5a). The distal boundary surrounded the most protruding portion of the tibial tubercle (Figure 5a). The medial boundary was easily distinguished from the pes anserinus. As the lateral boundary, some of the superficial fibres were continuous over the fascia of the tibialis anterior muscle. In the 3D analysis, the insertion site of the patellar tendon on the tibial side was crescent-shaped in the anterior view (Figure 5b); its surface area was 409.5 ± 96.9 mm^2 (range, 244.2–545.9 mm^2). The vertex of the arcuate groove of the tibia was 35.5 ± 2.8% of the distal width of the patellar tendon from its medial side (Figure 2a). Quantitative data are summarised in Table 1.

3.2. Three-dimensional measurement and analysis of the patellar tendon

3.2.1. Width of the patellar tendon

The proximal, central and distal widths were 29.9 ± 2.7 mm, 27.3 ± 2.5 mm and 25.0 ± 2.4 mm, respectively. The width of each portion varied significantly ($P < 0.05$). The patellar tendon was broad proximally but became narrow distally in all specimens. Quantitative data are summarised in Table 1.

3.2.2. Length of the patellar tendon

The patellar tendon was the shortest at 40.6 ± 6.7% of the central width from its medial edge. As measured at every 10% interval, the shortest length of the patellar tendon was 38.0 ± 4.1 mm or 40% of the central width from its medial edge. The longest length of the patellar tendon was 54.1 ± 6.8 mm or 90% of the central width from its medial edge. The length of each adjacent part varied significantly ($P < 0.05$) and gradually became longer toward both edges. The lateral length was always longer than the medial length when comparing the same portion from both edges. The mean measurements of the patellar tendon length at each position are presented in Figure 2b.

3.2.3. Thickness of the patellar tendon

The thickness of the central part of the patellar tendon did not significantly differ in the range of 40–75% from the medial edge ($P = 0.051$), and the average thickness in this range was 4.5 ± 0.6 mm. The patellar tendon gradually became thinner toward

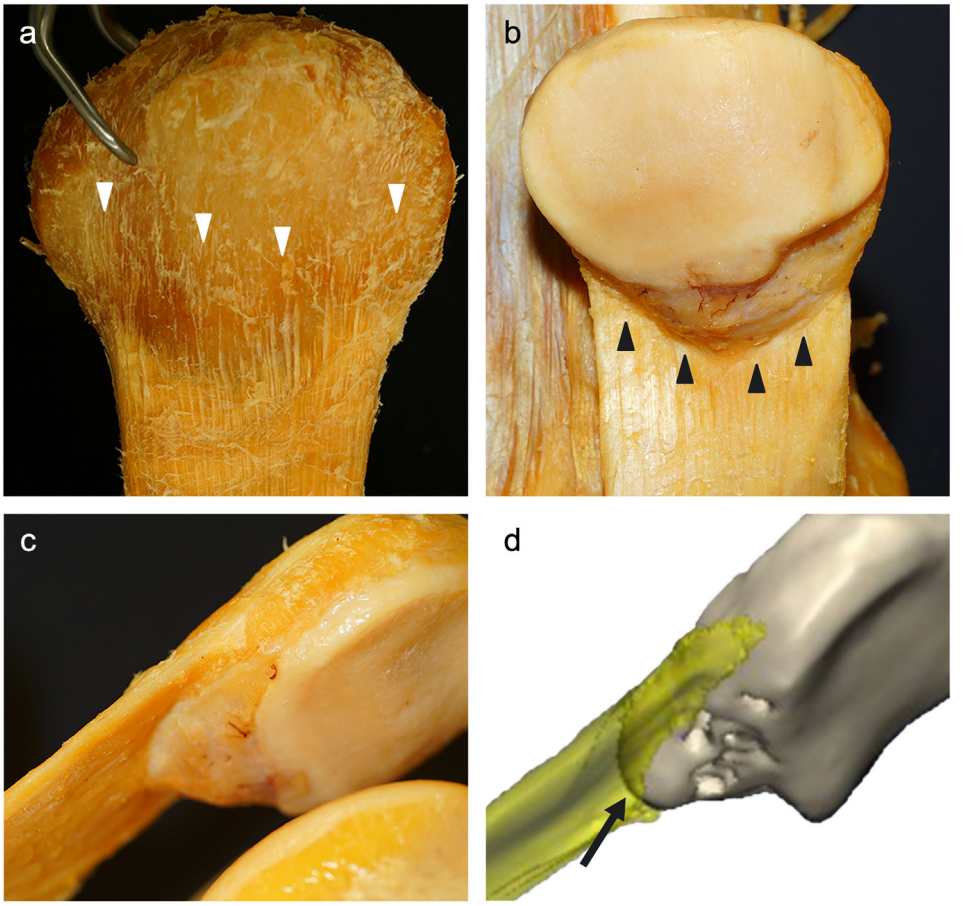

Figure 4. Photographs and three-dimensional image showing the patellar tendon insertion on the patellar side (left knee). a. Anterior view. The white arrowheads indicate anterior superficial fibres spreading over the patellar surface. b. Posterior view. The black arrowheads indicate posterior superficial fibres of the patellar tendon inserting on the inferior pole of the patella. c. Oblique view observed from the lateral side. It was difficult to observe the inferior patellar edge. d. Three-dimensional image showing that the line of the inferior patellar edge was surrounded by the patellar tendon. The black arrow indicates the apex of the inferior pole of the patella.

both edges. The mean measurements of the thickness of each portion of the central part of the patellar tendon are presented in Figure 3b.

4. Discussion

The most important finding of the present study was clarification of the morphology of the patellar tendon and both insertion sites based on 3D images. The varying regional morphology of the patellar tendon has intrinsic features in each portion. The insertion sites of the patellar and tibial sides were V-shaped and crescent-shaped, respectively, with their bony apexes both located slightly medial of the width of the tendon in all knees.

The present study provided detailed data concerning the regional lengths of the patellar tendon. The length of the patellar tendon was shortest at a location approximately 40% medial of the central width; the lateral side was longer than the medial side, which gradually became longer toward both edges. The length of the centre portion in the present study was similar or slightly shorter than that reported in previous studies that used a scale ruler in intraoperative measurements and biomechanical

Table 1
Patellar tendon width according to location and bony apex rate at the insertions.

	Proximal (patellar side)	Central	Distal (tibial side)
Patellar tendon width (mm)	29.9 ± 2.7 (26.5–36.7)	27.3 ± 2.5 (23.7–34.1)	25.0 ± 2.4 (21.3–30.9)
Bony apex rate (%)	44.5 ± 2.2 (39.3–49.2)	–	35.5 ± 2.8 (29.8–40.0)

Data are presented as mean ± standard deviation (range).

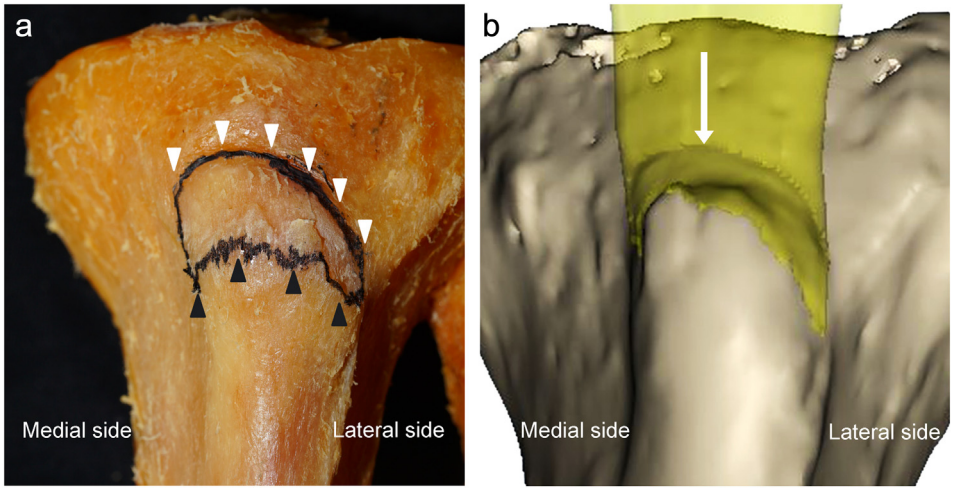

Figure 5. Photograph and three-dimensional image showing the patellar tendon insertion on the tibial side (left knee). a. Macroscopic image of an anterior view showing the insertion site of the patellar tendon on the tibial side, with the patellar tendon removed after computed tomographic scanning. The white arrowhead indicates the tibial arcuate groove. The black arrowhead indicates the distal boundary of the insertion site. b. Three-dimensional image of an anterior view showing the positional relationship of the arcuate groove and patellar tendon. The white arrow indicates the vertex of the arcuate groove. The insertion site on the tibial side was crescent-shaped.

research [20,31–35] or that used mid-sagittal MRI for pre-operative assessment of BTB ACL reconstruction [12,18,20,36,37]. However, previous studies measured the patellar tendon at only one location, and the variance in the regional length of the whole patellar tendon was not mentioned. Goldstein et al. showed that a correlation exists among the patient's height, sex, and patellar tendon length; to avoid graft–tunnel mismatch, they recommended the use of a tendon length less than or equal to the mean length for the sex-specific height subgroup to reduce the possibility of construct mismatch when applying an allograft [12]. To prevent mismatch when using an autograft, Chang et al. suggested pre-operative assessment using MRI to estimate the tendon length of a BTB graft [20]. The current findings that the length of the tendon shows marked variation in each portion should further aid in harvesting a graft with an appropriate length for BTB ACL reconstruction.

The present study also revealed the thickness of the patellar tendon at each location and showed that it was thick in the central portion of 40–75% and gradually became thinner toward both edges. Several previous studies have measured the thickness of the central portion using MRI or scale callipers [20,34,35,37]. Chang et al. reported that the mean thicknesses of the patellar tendon, using MRI, and intraoperative measurements were 3.9 mm and 3.8 mm, respectively, showing the accuracy and reliability of assessment using MRI [20]. Their results regarding the central thickness of the tendon were similar to those of the present study; however, they did not report the varying regional thickness of the entire patellar tendon [20]. Yanke et al. analysed graft geometry in their study of biomechanical properties comparing the 10-mm central third and 10-mm medial and lateral sides of a BTB graft [35]. Although there was no significant difference in the tendon thickness, width or length among graft types, the biomechanical failure properties of the central third of a BTB graft were superior to those of the other grafts [35]. However, considering the results of the current study using 3D images, it is possible that the tendon thickness varied among these grafts and influenced the graft strength, which is important when harvesting a graft for ACL reconstruction.

The current study revealed the morphology of the insertion site on both the patellar and tibial sides of the patellar tendon. The findings regarding the patellar insertion site of the patellar tendon were similar to the anatomical findings from the gross observations of Basso et al., who reported that the patellar bony apex was located at 39.0% of the width of the tendon from its medial edge, using a needle to identify the tip of the apex [21]. Tibial arcuate groove has been described in previous studies [38,39]. However, no studies have reported the detailed characteristics of the tibial insertion site, which might be difficult to measure and analyse using a macroscopic method. The present results, including the surface area regarding the tibial insertion site of the patellar tendon based on 3D images, are new findings and indicate that this area is consistent. They verified that the bony apexes of the insertion sites (V-shaped on the patellar side and crescent-shaped on the tibial side) were consistently located slightly medial of the width of the patellar tendon. This indicates that the characteristics of the BTB graft markedly depend on the location from which it is harvested.

A new method of BTB ACL reconstruction with an anatomic rectangular tunnel has been reported, whereby a single BTB graft is placed to mimic the natural fibre arrangement of the normal ACL following the concept of double-bundle reconstruction [22–25]. In these techniques, the graft is not harvested from the central portion of the patellar tendon. Hence, the tendinous portion of the graft has longer and shorter sides: the longer sides are assigned to the anteromedial portion of the graft and the shorter sides to the posterolateral portion. Furthermore, the bone plug, which is chosen for the femoral side, is shaped in accordance with the parallelepiped femoral tunnel with a rectangular aperture. The current study showed that the morphological features of the bone–tendon junctions of the BTB graft were rigidly characterised by the harvested site. This could aid in

considering not only the natural fibre arrangement of the normal ACL but also the shape of the bone–tendon junction of the femoral tunnel aperture.

The present study had several limitations. First, the cadavers were mostly elderly. Consequently, degenerative changes may have influenced the results. Second, the tissues were fixed in formalin. The change in tissue elasticity caused by the formalin solution may have influenced the results [40]. Third, although accurate 3D measurement was performed, the method depended on human dissection and decisions, which might have introduced bias. Fourth, relatively few cadavers were investigated, and normal anatomical variation cannot be ruled out. Fifth, the sex, physique, and ethnicity of the cadavers might have influenced the results.

The clinical relevance of the present study is that clarifications of the morphology of the patellar tendon and its insertion sites on both sides can help to predetermine the length, width and shape of the bone–tendon junctions of BTB grafts. The present findings will help surgeons to harvest an appropriate BTB graft, which is essential for successful ACL reconstruction.

5. Conclusion

The morphological properties of the patellar tendon and its insertion sites on both the patellar and tibial sides were consistent. These findings indicate that the characteristics of the BTB graft markedly depend on the location from which it is harvested.

Declarations of interest

None.

Funding

This work was supported by Japan Society for the Promotion of Science KAKENHI [grant number 15K01562].

Ethical approval

All procedures performed in studies involving human participants were in accordance with ethical standards of the institutional and/or national research committee and with the 1964 Helsinki declaration and its later amendments or comparable standards.

Informed consent

Informed consent was obtained from all individual participants included in this study.

Acknowledgements

The authors wish to thank Professors Jiro Hitomi and Yoichi Sato from the Department of Anatomy of Iwate Medical University for their continuous support of this study. We also thank Mr. Masayoshi Kamata from the Department of Radiology of Iwate Medical University Hospital for his technical assistance. We thank Kelly Zammit, BVSc, from Edanz Group (www.edanzediting.com/ac), for editing a draft of this manuscript.

References

[1] Heijne A, Hagstromer M, Werner S. A two- and five-year follow-up of clinical outcome after ACL reconstruction using BPTB or hamstring tendon grafts: a prospective intervention outcome study. Knee Surg Sports Traumatol Arthrosc 2015;23:799–807.
[2] Moller E, Weidenhielm L, Werner S. Outcome and knee-related quality of life after anterior cruciate ligament reconstruction: a long-term follow-up. Knee Surg Sports Traumatol Arthrosc 2009;17:786–94.
[3] Xie X, Liu X, Chen Z, Yu Y, Peng S, Li Q. A meta-analysis of bone–patellar tendon–bone autograft versus four-strand hamstring tendon autograft for anterior cruciate ligament reconstruction. Knee 2015;22:100–10.
[4] Noyes FR, Butler DL, Grood ES, Zernicke RF, Hefzy MS. Biomechanical analysis of human ligament grafts used in knee-ligament repairs and reconstructions. J Bone Joint Surg Am 1984;66:344–52.
[5] Schatzmann L, Brunner P, Staubli HU. Effect of cyclic preconditioning on the tensile properties of human quadriceps tendons and patellar ligaments. Knee Surg Sports Traumatol Arthrosc 1998;6(Suppl. 1):S56–61.
[6] Kurosaka M, Yoshiya S, Andrish JT. A biomechanical comparison of different surgical techniques of graft fixation in anterior cruciate ligament reconstruction. Am J Sports Med 1987;15:225–9.
[7] Grana WA, Egle DM, Mahnken R, Goodhart CW. An analysis of autograft fixation after anterior cruciate ligament reconstruction in a rabbit model. Am J Sports Med 1994;22:344–51.
[8] Berkson E, Lee GH, Kumar A, Verma N, Bach Jr BR, Hallab N. The effect of cyclic loading on rotated bone–tendon–bone anterior cruciate ligament graft constructs. Am J Sports Med 2006;34:1442–9.
[9] Shaffer B, Gow W, Tibone JE. Graft-tunnel mismatch in endoscopic anterior cruciate ligament reconstruction: a new technique of intraarticular measurement and modified graft harvesting. Art Ther 1993;9:633–6.
[10] Spindler KP, Bergfeld JA, Andrish JT. Intraoperative complications of ACL surgery: avoidance and management. Orthopedics 1993;16:425–30.
[11] Verma N, Dennis MG, Carreira DS, Bojchuk J, Hayden JK, Bach Jr BR. Preliminary clinical results of two techniques for addressing graft tunnel mismatch in endoscopic anterior cruciate ligament reconstruction. J Knee Surg 2005;18:183–91.

[12] Goldstein JL, Verma N, McNickle AG, Zelazny A, Ghodadra N, Bach Jr BR. Avoiding mismatch in allograft anterior cruciate ligament reconstruction: correlation between patient height and patellar tendon length. Art Ther 2010;26:643–50.
[13] Auge II WK, Yifan K. A technique for resolution of graft–tunnel length mismatch in central third bone–patellar tendon–bone anterior cruciate ligament reconstruction. Art Ther 1999;15:877–81.
[14] Cooper DE. Biomechanical properties of the central third patellar tendon graft: effect of rotation. Knee Surg Sports Traumatol Arthrosc 1998;6(Suppl. 1):S16–9.
[15] Gerich TG, Cassim A, Lattermann C, Lobenhoffer HP. Pullout strength of tibial graft fixation in anterior cruciate ligament replacement with a patellar tendon graft: interference screw versus staple fixation in human knees. Knee Surg Sports Traumatol Arthrosc 1997;5:84–8.
[16] Miller MD, Hinkin DT. The "N + 7 rule" for tibial tunnel placement in endoscopic anterior cruciate ligament reconstruction. Art Ther 1996;12:124–6.
[17] Verma N, Noerdlinger MA, Hallab N, Bush-Joseph CA, Bach Jr BR. Effects of graft rotation on initial biomechanical failure characteristics of bone–patellar tendon–bone constructs. Am J Sports Med 2003;31:708–13.
[18] Brown JA, Brophy RH, Franco J, Marquand A, Solomon TC, Watanabe D, et al. Avoiding allograft length mismatch during anterior cruciate ligament reconstruction: patient height as an indicator of appropriate graft length. Am J Sports Med 2007;35:986–9.
[19] Olszewski AD, Miller MD, Ritchie JR. Ideal tibial tunnel length for endoscopic anterior cruciate ligament reconstruction. Art Ther 1998;14:9–14.
[20] Chang CB, Seong SC, Kim TK. Preoperative magnetic resonance assessment of patellar tendon dimensions for graft selection in anterior cruciate ligament reconstruction. Am J Sports Med 2009;37:376–82.
[21] Basso O, Johnson DP, Amis AA. The anatomy of the patellar tendon. Knee Surg Sports Traumatol Arthrosc 2001;9:2–5.
[22] Hayashi H, Kurosaka D, Saito M, Ikeda R, Kijima E, Yamashita Y, et al. Anterior cruciate ligament reconstruction with bone–patellar tendon–bone graft through a rectangular bone tunnel made with a rectangular retro-dilator: an operative technique. Arthrosc Tech 2017;6:e1057–62.
[23] Shino K, Mae T, Tachibana Y. Anatomic ACL reconstruction: rectangular tunnel/bone–patellar tendon–bone or triple-bundle/semitendinosus tendon grafting. J Orthop Sci 2015;20:457–68.
[24] Shino K, Nakata K, Nakamura N, Toritsuka Y, Horibe S, Nakagawa S, et al. Rectangular tunnel double-bundle anterior cruciate ligament reconstruction with bone–patellar tendon–bone graft to mimic natural fiber arrangement. Art Ther 2008;24:1178–83.
[25] Shino K, Nakata K, Nakamura N, Toritsuka Y, Nakagawa S, Horibe S. Anatomically oriented anterior cruciate ligament reconstruction with a bone–patellar tendon–bone graft via rectangular socket and tunnel: a snug-fit and impingement-free grafting technique. Art Ther 2005;21:1402.
[26] Suzuki T, Shino K, Nakagawa S, Nakata K, Iwahashi T, Kinugasa K, et al. Early integration of a bone plug in the femoral tunnel in rectangular tunnel ACL reconstruction with a bone–patellar tendon–bone graft: a prospective computed tomography analysis. Knee Surg Sports Traumatol Arthrosc 2011;19 (Suppl. 1):S29–35.
[27] Bi C, Ji X, Wang F, Wang D, Wang Q. Digital anatomical measurements and crucial bending areas of the fixation route along the inferior border of the arcuate line for pelvic and acetabular fractures. BMC Musculoskelet Disord 2016;17:125.
[28] Han L, Long T, Tang W, Liu L, Jing W, Tian WD, et al. Correlation between condylar fracture pattern after parasymphyseal impact and condyle morphological features: a retrospective analysis of 107 Chinese patients. Chin Med J (Engl) 2017;130:420–7.
[29] Park SB, An SY, Han WJ, Park JT. Three-dimensional measurement of periodontal surface area for quantifying inflammatory burden. J Periodontal Implant Sci 2017;47:154–64.
[30] Gelaude F, Vander Sloten J, Lauwers B. Accuracy assessment of CT-based outer surface femur meshes. Comput Aided Surg 2008;13:188–99.
[31] Denti M, Bigoni M, Randelli P, Monteleone M, Cevenini A, Ghezzi A, et al. Graft-tunnel mismatch in endoscopic anterior cruciate ligament reconstruction. Intraoperative and cadaver measurement of the intra-articular graft length and the length of the patellar tendon. Knee Surg Sports Traumatol Arthrosc 1998;6:165–8.
[32] Luk KM, Wong NM, Cheng JC. Anthropometry of the patellar tendon in Chinese. J Orthop Surg (Hong Kong) 2008;16:39–42.
[33] Navali AM, Jafarabadi MA. Is there any correlation between patient height and patellar tendon length? Arch Bone Jt Surg 2015;3:99–103.
[34] Yanke A, Bell R, Lee A, Shewman EF, Wang V, Bach Jr BR. Regional mechanical properties of human patellar tendon allografts. Knee Surg Sports Traumatol Arthrosc 2015;23:961–7.
[35] Yanke A, Bell R, Lee A, Shewman EF, Wang V, Bach Jr BR. Central-third bone–patellar tendon–bone allografts demonstrate superior biomechanical failure characteristics compared with hemi-patellar tendon grafts. Am J Sports Med 2013;41:2521–6.
[36] Wang H, Hua C, Cui H, Li Y, Qin H, Han D, et al. Measurement of normal patellar ligament and anterior cruciate ligament by MRI and data analysis. Exp Ther Med 2013;5:917–21.
[37] Yoo JH, Yi SR, Kim JH. The geometry of patella and patellar tendon measured on knee MRI. Surg Radiol Anat 2007;29:623–8.
[38] Ehrenborg G, Engfeldt B. The insertion of the ligamentum patellae on the tibial tuberosity. Some views in connection with the Osgood–Schlatter lesion. Acta Chir Scand 1961;121:491–9.
[39] Hughes ES, Sunderland S. The tibial tuberosity and the insertion of the ligamentum patellae. Anat Rec 1946;96:439–44.
[40] Ling Y, Li C, Feng K, Duncan R, Eisma R, Huang Z, et al. Effects of fixation and preservation on tissue elastic properties measured by quantitative optical coherence elastography (OCE). J Biomech 2016;49:1009–15.